Minimal RNA Constructs That Specifically Bind Aminoglycoside Antibiotics with High Affinities†

Keita Hamasaki, Jennifer Killian, Junhyeong Cho, and Robert R. Rando*

Department of Biological Chemistry and Molecular Pharmacology, Harvard Medical School, 250 Longwood Avenue, Boston, Massachusetts 02115

Received May 9, 1997; Revised Manuscript Received August 13, 1997⊗

ABSTRACT: RNA molecules are the functional targets for aminoglycosides. In order to approach an understanding of the rules which underlie aminoglycoside−RNA recognition, high-affinity RNA aptamers have been prepared which discriminate among various aminoglycosides [Wang et al. (1996) *Biochemistry 35*, 12338−12346]. One of these aptamers, J6, which is 109 nts in length, binds the aminoglycoside tobramycin stoichiometrically with a dissociation constant of 0.77 ± 0.03 nM. Aminoglycosides, similar in structure to tobramycin, bind with affinities diminished by 10^3-10^4 compared to tobramycin. Experiments are reported here which are designed to reveal the nature of the tobramycin binding domain of J6. A small (40 nts) stem−loop derivative of J6, containing a 3 nt and a 1 nt bulge, stoichiometrically binds tobramycin with a dissociation constant of approximately 5 nM. This construct can strongly discriminate between similar aminoglycosides with respect to binding. Elimination of either the three or the single nucleotide bulge eliminates specific aminoglycoside binding. The structure of the loop region is also critical. These studies demonstrate that simplified RNA molecules can be generated which bind aminoglycosides specifically and with high affinities.

Aminoglycoside antibiotics are thought to function in large part by binding to the decoding region of bacterial 16S rRNA (Noller, 1991; DeStasio & Dahlberg, 1990). The binding of aminoglycosides to this region can cause premature termination and mistranslation of proteins and, consequently, bacterial death (Chambers & Sande, 1996; Purohit & Stern, 1994; Noller, 1991). The binding of aminoglycosides to the decoding region is not a highly specific affair. First, binding affinities are relatively modest, being in the micromolar range (Noller, 1991; Wang et al., 1997). Moreover, there is not a great deal of selectivity evident with respect to the structures of the aminoglycosides that bind (Noller, 1991; Purohit & Stern, 1994; Wang et al., 1997). Indeed, high-field NMR studies on the structure of a complex formed between aminoglycosides and a truncated, low-affinity, decoding region construct show that a substantial portion of the aminoglycoside structure is not even involved in interactions with the RNA molecule (Fourmy et al., 1996). Aminoglycoside antibiotics have also been found to inhibit group I intron splicing by binding at specific RNA sites (von Ahsen et al., 1991, 1993). Like the 16S decoding region, little specificity is evident with respect to aminoglycoside structure.

† These studies were partially funded by U.S. Public Health Service National Institutes of Health Grants EY-03624 and EY-04096. J.K. was funded by Postdoctoral Fellowship EY-06634 and K.H. by a research fellowship from the Japan Society for the Promotion of Science.

* To whom correspondence should be addressed.

⊗ Abstract published in *Advance ACS Abstracts,* October 1, 1997.

An understanding of the rules underlying RNA−aminoglycoside recognition would be extremely useful as a basis for the design of potent and selective antagonists of RNA function. One approach to this problem involves the selection and characterization of high-affinity RNA molecules able to specifically recognize a particular aminoglycoside (Wang & Rando, 1995; Lato et al., 1995; Wallis et al., 1995). If the specific aminoglycoside-binding RNA molecules (aptamers) are simple (small) enough, their structures can be determined spectroscopically.

Previously, we reported on the selection of RNA aptamers which were directed against the aminoglycoside tobramycin (Scheme 1) (Wang & Rando, 1995; Wang et al., 1996). By selecting under stringent conditions, tobramycin aptamers were found that bound tobramycin with subnanomolar dissociation constants, and discriminated among similar aminoglycosides with respect to binding (Wang & Rando, 1995; Wang et al., 1996). One of these aptamers, J6 (Scheme 2), bound stoichiometrically to tobramycin with a $K_D = 0.77 + 0.03$ nM, while binding to similar aminoglycosides with K_D values 10^3-10^4 times higher (Wang & Rando, 1995; Wang et al., 1996). Affinity cleavage studies also demonstrated that the aminoglycoside binding site of J6 involves the stem−loop consensus region, identified in Scheme 2 (Wang et al., 1996). An important question to answer is how much of the full J6 construct is important for both high-affinity and specific aminoglycoside binding. Obtaining minimally sized high-affinity constructs is also important for possible structural determination. In the work reported here, it is shown that the 109 nt J6 aptamer can be

S0006-2960(97)01095-7 CCC: $15.00
Published on Web 01/13/1998

Scheme 1: Aminoglycosides Used in the Binding Assays

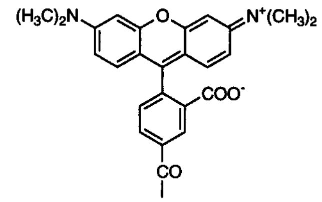

TR- : 5-carboxytetramethylrhodamine

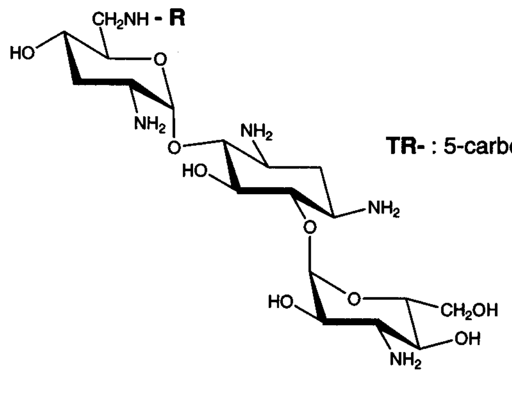

Tobramycin (R = H)
CRT (R = TR)

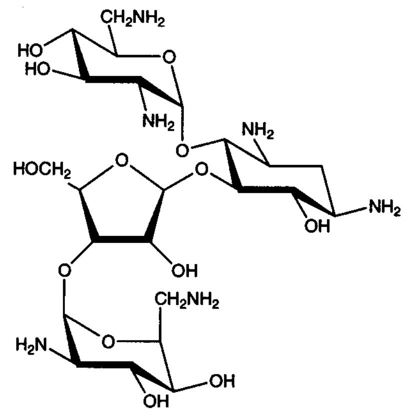

Neomycin B

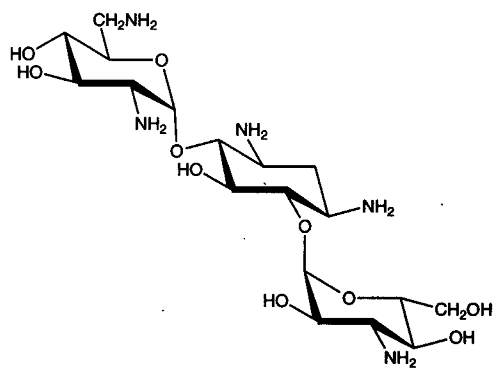

Kanamycin B

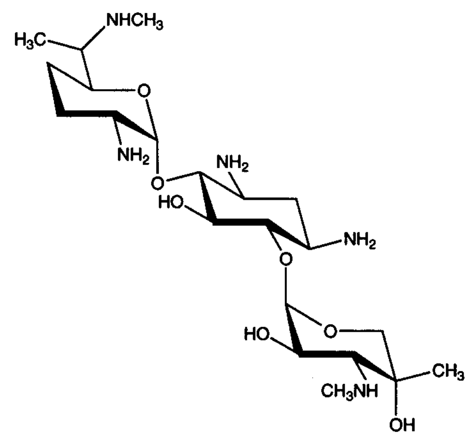

Gentamycin C1

simplified to 39 nt length aptamers without substantial loss of affinity and specificity with respect to tobramycin binding.

MATERIALS AND METHODS

Materials

Kanamycin B was from Sigma. Neomycin, tobramycin, and gentamycin were purchased from Fluka. 5-Carboxytetramethylrhodamine succinimidyl ester was purchased from Molecular Probes, Inc. or IDT. 5-Carboxytetramethylrhodamine-labeled tobramycin (CRT) was prepared as previously reported (Wang et al., 1996). The restriction enzymes *Mbo*I, *Ava*II, and *Nde*I were purchased from Promega, Inc. Oligonucleotides were obtained from Oligo's, Etc., Inc. PCR reactions were carried out using the Gene Amp PCR kit with AmpliTaq DNA polymerase from Perkin Elmer. RT/PCR was carried out using the Gene Amp Thermostable r*Tth* reverse transcriptase RNA PCR kit from Perkin Elmer. RNA transcripts were generated using the T7 MEGAshortscript kit from Ambion or the RiboMAX large-scale RNA production kit with T7 RNA polymerase from Promega. *N*-Hydroxysuccinimide-derivatized Affi-Gel 10 was from Bio-Rad. Sephadex G-50 was from Pharmacia. Cloning was carried out using the Original TA Cloning kit from Invitrogen. Plasmid DNA was purified using the Wizard Miniprep DNA purification system from Promega. RNase T1 and RNase U2 were obtained from U.S. Biochemicals, Inc.

Methods

RNase Cleavage of J6 RNA. 5′-^{32}P-labeled J6 RNA (20 kcpm) was refolded in 40 μL of 150 mM NaCl, 5 mM KCl, 1 mM $CaCl_2$, 1 mM $MgCl_2$, and 20 mM HEPES (pH 7.4). The appropriate dilution of either RNase T1 or RNase U2 was added, and the mixture was incubated for 4 min at 25 °C. The reaction was stopped by addition of a 3 M sodium acetate solution containing 25 mM EDTA, and then precipitated with ethanol. Electrophoresis was carried out for 2 h on an 8% polyacrylamide gel.

Preparation of J6 RNA Analogs. The template DNAs for J6a, J6b, and J6c were generated by restriction enzyme digestion based on the original template DNA for J6 (*Nde*I, *Ave*I, and *Mbo*I for J6a, J6b, and J6c, respectively). The restriction enzyme digests were carried out using the corresponding buffer provided with the enzyme. The digests were carried out at 37 °C for 2 h. The digestion reactions were followed by gel analysis using 13% polyacrylamide gel electrophoresis. The crude digestion mixtures were used as

Scheme 2: Secondary Structure Plot of J6 RNA[a]

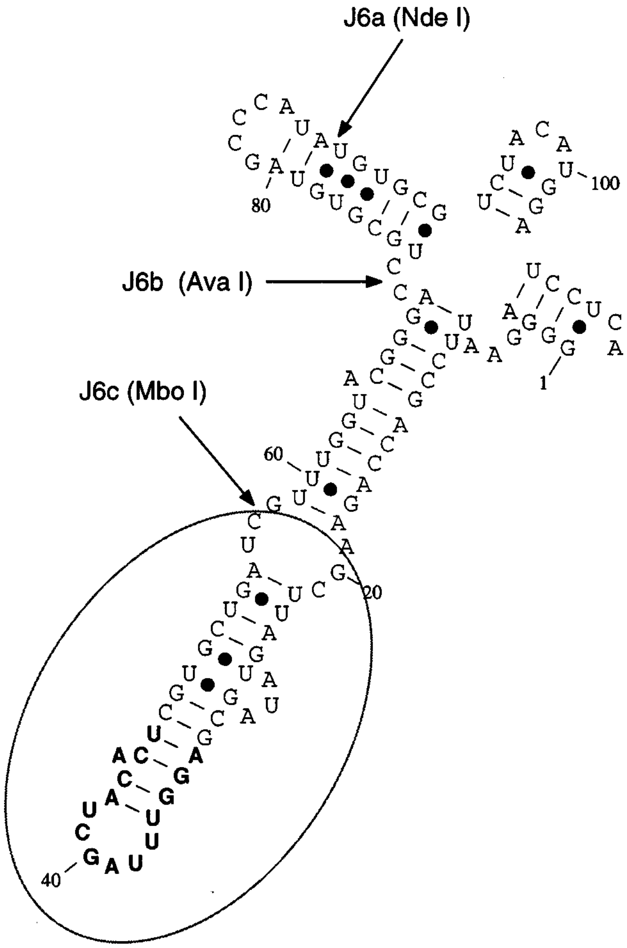

[a] The outlined area contains the structure of the putative aminoglycoside binding domain. The arrows indicate the restriction sites, and the lengths of the RNA transcription runoffs. The consensus region is indicated in boldface type.

Scheme 3: Enzymatic Cleavages Pattern in J6 RNA[a]

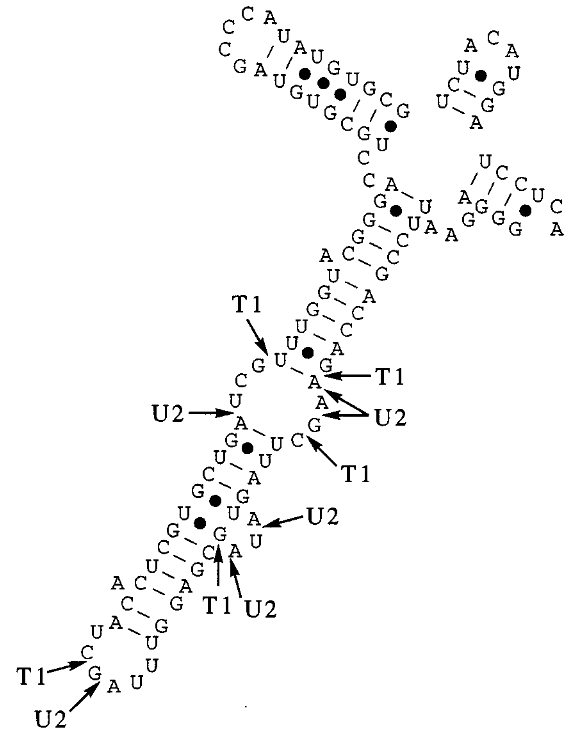

[a] The cleavage sites by RNase T1 and RNase U2 are indicated.

templates. The template DNAs for J6e's and J6f's were purchased from Oligo's, Etc., Inc. and used without further purification. Each template DNA has an additional G residue on the 5′-terminal or G-C base pair for the sake of increasing enzymatic transcription efficiency (Aziz & Soreq, 1990) and/or whole RNA structural stability. Double-stranded DNA templates were successfully prepared by PCR. Each RNA was generated by T7 RNA polymerase, and then purified using a NICK Sephadex G-50 column to remove unincorporated mononucleotides.

Fluorescence Measurements. Tetramethylrhodamine labeled tobramycin (CRT) concentrations were determined spectroscopically at 550 nm using a molar extinction coefficient of 6.00×10^4 M^{-1} cm^{-1}. Fluorescence anisotropy measurements were performed on a Perkin Elmer LS-50B luminescence spectrometer equipped with a thermostat accurate to + 0.1 °C. The tracer solution was excited at 550 nm, and monitored at 580 nm. The integration time was 5 s. For every single point, six measurements were made, and their average values were used for calculation. Measurements were performed in buffer solution containing 140 mM NaCl, 5 mM KCl, 1 mM $MgCl_2$, 1 mM $CaCl_2$, and 20 mM HEPES (pH 7.5).

Determination of Dissociation Constants. The following equation (Wang & Rando, 1995) was used for the determination of the dissociation constant for the interactions between RNA and CRT (K_d):

$$A = A_0 + \Delta A\,\{([\mathrm{RNA}]_0 + [\mathrm{CRT}]_0 + K_d) - [([\mathrm{RNA}]_0 + [\mathrm{CRT}]_0 + K_d)^2 - 4[\mathrm{RNA}]_0[\mathrm{CRT}]_0]^{1/2}\}/2 \quad (1)$$

where A and A_0 are the fluorescence anisotropy of CRT in the presence and in the absence of RNA, respectively, ΔA is the difference between the fluorescence anisotropy of 1 nM CRT in the presence of an infinite concentration of RNA minus the fluorescence anisotropy in the absence of RNA. $[\mathrm{RNA}]_0$ and $[\mathrm{CRT}]_0$ are the initial concentrations of RNA and CRT, respectively.

In the competitive binding assay, eq 2 (Wang et al., 1996) is used for the calculation of the K_D values:

$$[\mathrm{aminoglycoside}]_0 = \{K_D(A_\infty - A)/[K_d(A - A_o) + 1]\} \times \{[\mathrm{RNA}]_0 - K_d(A - A_o)/(A_\infty - A) - [\mathrm{CRT}]_0(A - A_o)/(A_\infty - A_o)\} \quad (2)$$

where K_D is the dissociation constant between the RNA and the aminoglycosides and $[\mathrm{aminoglycoside}]_0$ is the initial concentration of the aminoglycosides. Both K_d and K_D were determined by non linear curve-fitting using the equations described above (Wang et al., 1996).

RESULTS

Enzymatic Probing of the Secondary Structure of J6. Before initiating experiments to probe the minimal aminoglycoside binding unit of J6, further evidence was sought for the proposed secondary structure of J6 (Scheme 2). Previously it had been shown that tobramycin-based affinity cleaving agents specifically cleave J6 in the stem−loop region, a region thought to contain the tobramycin binding

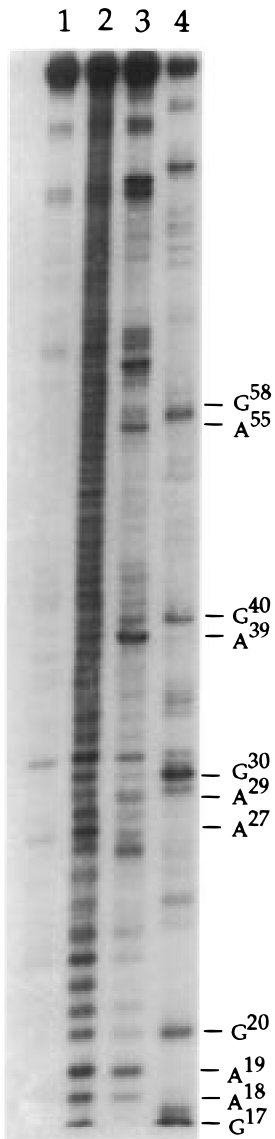

FIGURE 1: RNase T1 and U2 cleavage of J6 RNA. Autoradiogram of an 8% denaturing polyacrylamide gel showing enzymatic cleavages of J6 RNA. (Lane 1) Intact J6 RNA; (lane 2) alkaline hydrolysis; (lane 3) RNase U2; (lane 4) RNase T1. All reactions contain 20 kcpm of J6 RNA, 150 mM NaCl, 5 mM KCl, 1 mM $CaCl_2$, 1 mM $MgCl_2$ and 20 mM HEPES (pH 7.4).

site (Wang et al., 1996). Further studies on J6 were carried out using RNase T1 and RNase U2 digests to probe the secondary structure of J6 RNA. RNase T1 is known to cleave RNA at unpaired G residues, and RNase U2 to cleave RNA at unpaired A residues. On the basis of the putative structure of J6 RNA, RNase T1 and RNase U2 are expected to cut the RNA in the bulge and loop regions. As shown in Scheme 3 and Figure 1, RNase T1 readily cleaves the J6 RNA at G58, G40, G30, G20, and G17. In contrast, while RNase U2 strongly cuts the RNA at A55, A39, and A19, weak cleavages by RNase U2 are observed at A29, A27, and A18. No cleavage at the single bulged A45 is observed. These results are consistent with the Mfold predicted secondary structure of J6.

Restriction Enzyme Digests of J6 DNA. In order to uncover the minimal tobramycin binding domain of J6 RNA, restriction digests were carried out on the corresponding DNA construct, followed by runoff transcription of the DNA

Scheme 4: Secondary Structure Plots of J6c, J6d, and J6e

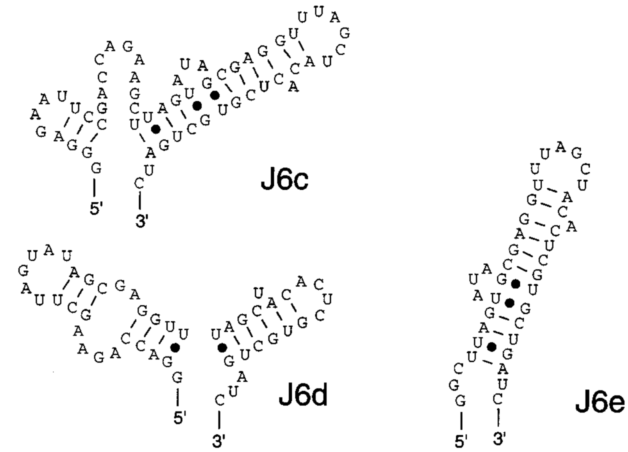

Table 1: Dissociation Constants between J6 Derivatives and CRT or Tobramycin

	CRT K_d (nM)	tobramycin K_D (nM)
J6 (109-mer)	12.2 + 1.1	0.77 + 0.03
J6a (87-mer)	383 + 67	14.4 + 1.5
J6b (71-mer)	708 + 80	31.8 + 7.1
J6c (57-mer)	732 + 91	25.0 + 1.2
J6d (47-mer)	nb[a]	−
J6e (39-mer)	546 + 76	58.2 + 13.1
J6e1 (40-mer)	291.4 + 19.4	15.6 + 1.5
J6e2 (37-mer)	ns[b]	−
J6f1 (40-mer)	192.6 + 11.1	5.15 + 1.52
J6f2 (37-mer)	ns	−
J6f3 (39-mer)	ns	−
J6f4 (40-mer)	ns	−
J6f5 (40-mer)	ns	−

[a] nb: no binding. [b] ns: nonstoichiometric binding.

fragments to generate truncated versions of J6. Quantitative binding measurements on the truncated J6 molecules were then performed to determine their specificities and affinities of aminoglycoside binding. Restriction cleavage sites for J6 are shown in Scheme 2. The consensus region is indicated in this scheme, as are the expected cleavage sites for the various restriction enzymes. Three restriction enzymes, *Nde*I (which generates an 87-mer-J6a), *Ava*II (which generates a 71-mer-J6b), and *Mbo*I (which generates a 57-mer-J6c), were chosen for study (Schemes 2 and 4). None of these restriction enzymes cut from the T7 promoter site through the consensus region. After digestion, RNA run offs were prepared, purified, and studied with respect to aminoglycoside binding. Binding was determined by fluorescence anisotropy measurements using the 5-carboxytetramethylrhodamine-labeled tobramycin (CRT) (Scheme 1), as previously reported (Wang et al., 1996). In the presence of an RNA construct that specifically binds to CRT, an increase in fluorescence anisotropy is observed, which yields the stoichiometry of binding as well as the dissociation constant for the binding reaction (Wang & Rando, 1995; Wang et al., 1996). The same quantitative information can be obtained for other aminoglycosides that bind to a particular RNA construct simply by performing competition experiments with CRT (Wang et al., 1996).

Binding of Aminoglycosides to J6 and Analogs Derived from Restriction Digests. Scheme 4 shows the Mfold-predicted (Jaeger et al., 1989) secondary structures of some of the J6 RNA derivatives generated by the use of the

Table 2: Binding Specificity of J6 RNA and Its Derivatives

	K_D (μM)			
aminoglycosides	J6 (109-mer)	J6c (57-mer)	J6e (39-mer)	J6f1 (40-mer)
tobramycin	0.00077 ± 0.00003	0.025 ± 0.0012	0.0582 ± 0. 0131	0.00515 ± 0.00042
kanamycin B	0.760 ± 0.016	0.872 ± 0.222	ns[a]	0.022 ± 0.0047
neomycin	1.03 ± 0.03	20.6 ± 3.5	35.1 ± 5.2	5.59 ± 1.39
gentamycin	7.81 ± 0.54	157 ± 19	nb[b]	43.7 ± 11.7

[a] ns: nonstoichiometric binding. [b] nb: no binding.

Scheme 5: Secondary Structure Plots of J6e1 and J6e2

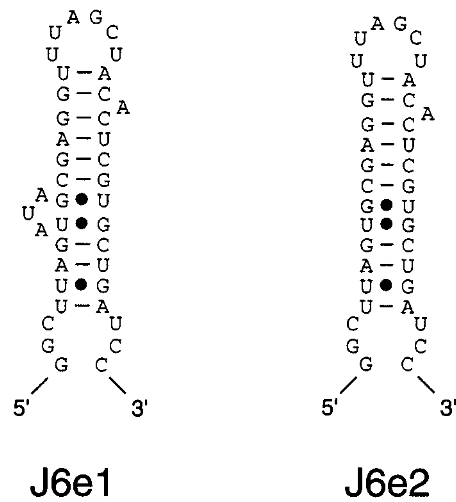

restriction enzymes described above. These constructs (Scheme 4) were then tested for binding to CRT as well as tobramycin. As shown in Table 1, in general there was a decrease in binding affinity as the constructs were simplified with respect to the binding of both CRT and tobramycin. Restriction cleavage from the 3′ end of the molecule did not practically allow for the preparation of molecules shorter than 57 nts long. Two further deletions from the 5′ end of the 57-mer (J6c) led to a 47-mer (J6d) and a 39-mer (J6e) (Scheme 4). When tested for antibiotic binding, J6d proved to lack aminoglycoside binding capacity, while J6c showed substantial affinities for CRT and tobramycin (Table 1). It is interesting to note that J6d was predicted to have a secondary structure quite unlike the other stem−loop structures hitherto investigated.

Some of the analogs were tested with respect to how specifically they were able to discriminate between various aminoglycosides (Table 2). It is remarkable that J6 itself discriminates so well among similar aminoglycosides. For example, kanamycin B only differs from tobramycin by the addition of a single hydroxyl group to ring 1 (Scheme 1). The 39-mer J6e showed substantial affinity for CRT and also was able to markedly discriminate between very similar aminoglycosides, as shown in Table 2. J6e was consequently investigated further in order to identify those structural elements essential for high-affinity and specific aminoglycoside binding.

Binding of Aminoglycosides to Analogs of J6e. Further studies in the J6e series were performed in order to maximize aminoglycoside binding affinities and specificity of binding. J6e1 and J6e2 (Scheme 5) were prepared to study the effect of terminal G-C pairing, and to determine whether the AUA trinucleotide bulge is important for binding. J6f's (Scheme 6) were prepared to determine the importance of the bulges

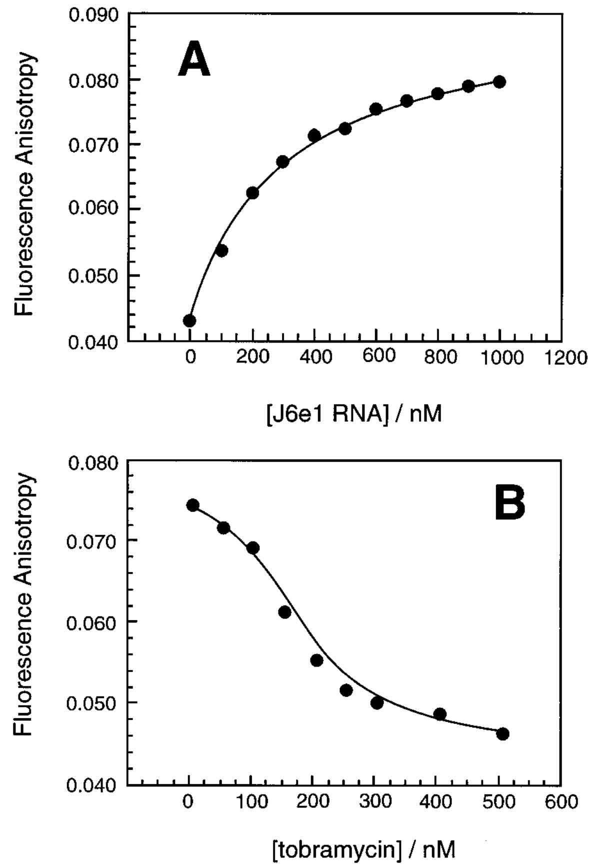

FIGURE 2: (A) Fluorescence anisotropy of CRT (10 nM) solution as a function of J6e1 RNA concentration. (B) Fluorescence anisotropy of CRT (10 nM) solution containing J6e1 RNA (500 nM) as a function of tobramycin concentration.

or the loop with respect to their abilities to bind aminoglycosides. Figures 2−6 show the binding curves for the five RNA constructs, and Table 1 summarizes the binding data for CRT and tobramycin. Interestingly, the additional GC base pair at the termini of the RNA constructs (J6e1 vs J6e) increases the affinity for tobramycin as shown in Table 1. Elimination of the trinucleotide bulge of J6e1 to produce J6e2 shows that the trinucleotide bulge is essential for high-affinity and specific aminoglycoside binding (Figure 3). The C for U point mutation in J6e1 generates J6f1 which shows high affinity and specific aminoglycoside binding. J6f1 binds tobramycin with a $K_D = 5.15 \pm 1.52$ nM, which is only less than 7-fold lower in affinity than the full J6 construct. The specificities of aminoglycoside binding to J6c, J6e, and J6f1 were compared to that of J6 itself (Table 2), which can differentiate by approximately 1000-fold between tobramycin and kanamycin B. Further studies in the J6f series (J6f2 and J6f3) show that both the three base bulge and the single A bulge moieties in the stem−loops are essential for specific aminoglycoside binding, because J6f2 and J6f3 show only

Scheme 6: Secondary Structure Plots of J6f1, J6f2, J6f3, J6f4, and J6f5

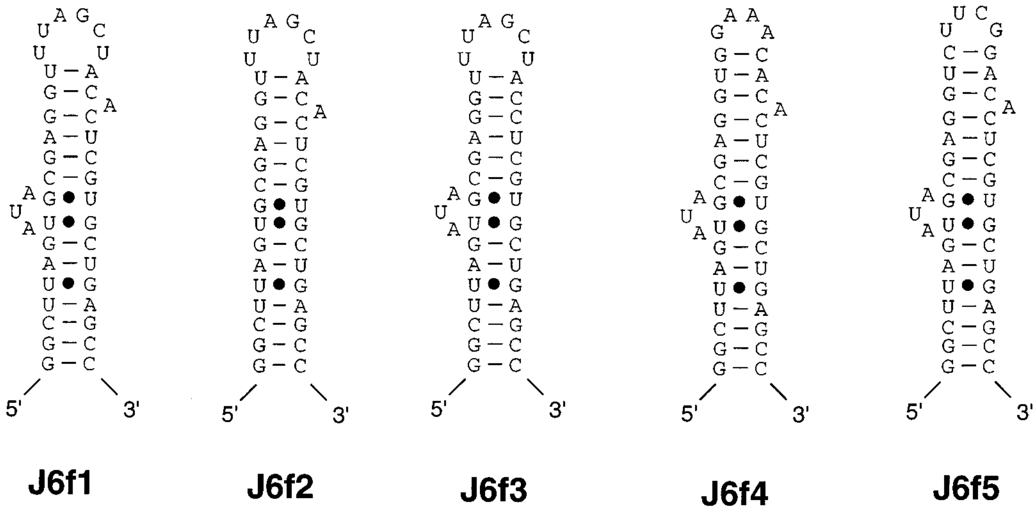

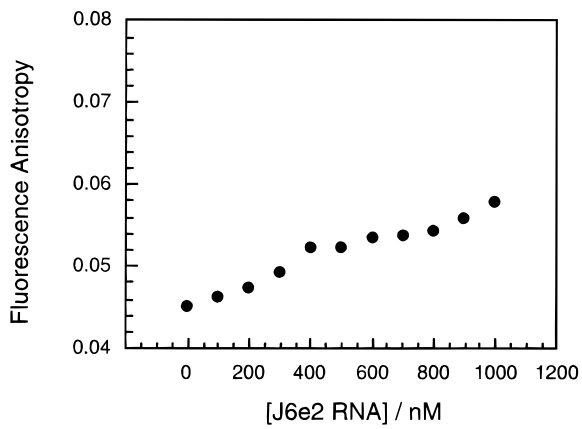

FIGURE 3: Fluorescence anisotropy of CRT (10 nM) solution as a function of J6e2 RNA concentration.

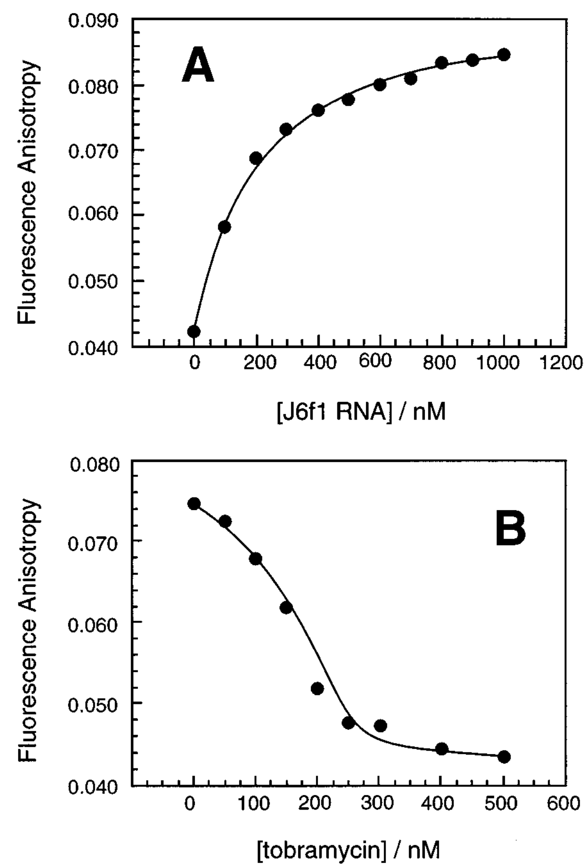

FIGURE 4: (A) Fluorescence anisotropy of CRT (10 nM) solution as a function of J6f1 RNA concentration. (B) Fluorescence anisotropy of CRT (10 nM) solution containing J6f1 RNA (500 nM) as a function of tobramycin concentration.

weak, nonsaturable aminoglycoside binding (only the data for J6f3 are shown in Figure 6A). The importance of the loop structure in J6 was probed by performing binding experiments on J6f4 and J6f5 (Scheme 6). J6f4 and J6f5 RNA constructs have standard four-base loops instead of the original six-base loop of J6. Both J6f4 and J6f5 show weak, nonstoichiometric binding (only the data for J6f5 are shown in Figure 6B).

DISCUSSION

The major reason for carrying out the kinds of experiments described here is to determine what the minimal RNA recognition units are which underlay specific, high-affinity, aminoglycoside binding. When tobramycin was used to select for RNA aptamers which could bind this aminoglycoside, it was noted that there were a vast number of nonconsensus, primary sequence solutions which were able to bind tobramycin with low micromolar affinities (Wang & Rando, 1995). Starting with approximately 10^{13} randomized RNA sequences, approximately 10^{7} sequences bound tobramycin with micromolar affinities (Wang & Rando, 1995). This shows that RNA molecules with micromolar affinities for aminoglycosides are readily obtained, and that particular, specific RNA structures are not required to achieve this relatively low level of affinity. Hence, studying RNA molecules which bind aminoglycosides with micromolar affinities would not likely provide discrete and interesting solutions with respect to RNA−aminoglycoside recognition. Therefore, high-affinity aptamers which bind aminoglycosides were sought to uncover more unique binding solutions.

Higher stringency selections led to the discovery of low nanomolar affinity binders of tobramycin in which clear consensus sequences were observed, suggesting that there were no further solutions for tight binding aptamers in the original pool (Wang & Rando, 1995). It is these tight binding aptamers which we find most interesting with respect

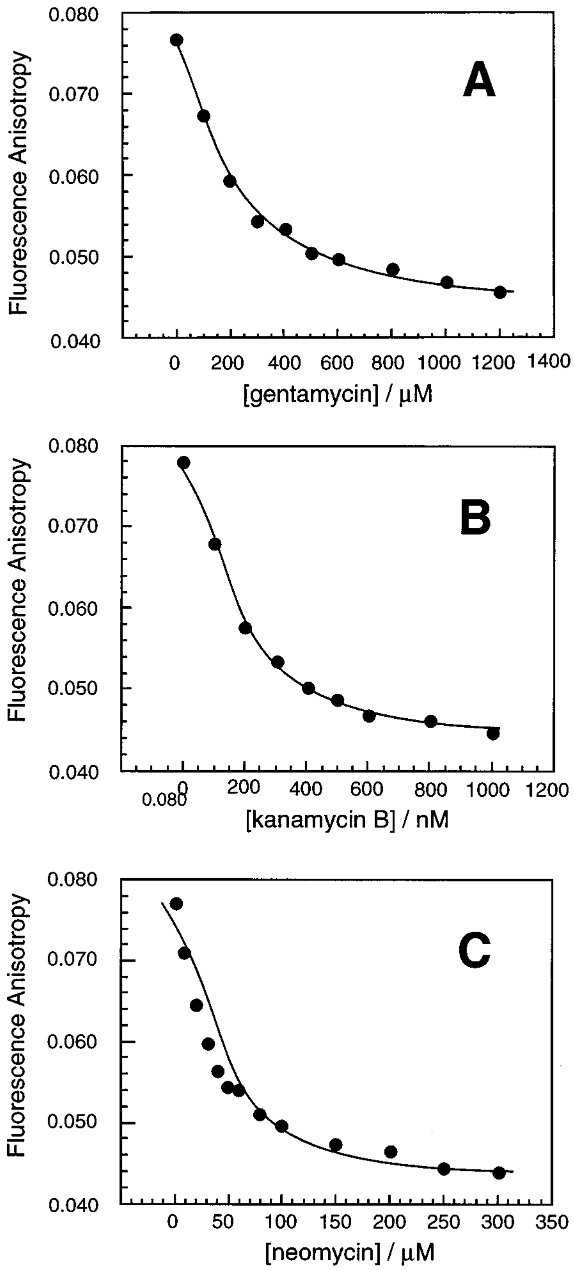

FIGURE 5: Fluorescence anisotropy of CRT (10 nM) solution containing J6f1 RNA (500 nM) as a function of gentamycin (A), kanamycin B (B), and neomycin (C) concentration.

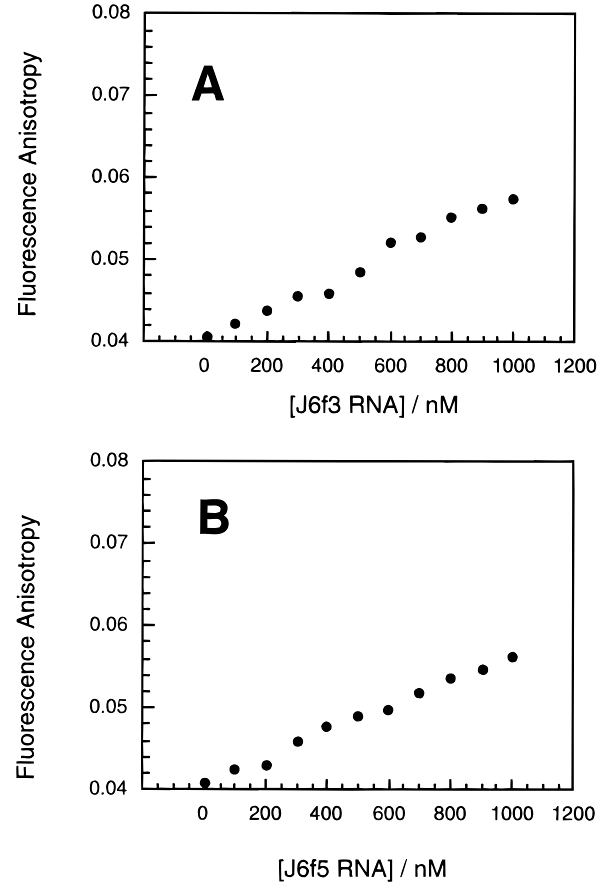

FIGURE 6: (A) Fluorescence anisotropy of CRT (10 nM) solution as a function of J6f3 RNA concentration. (B) Fluorescence anisotropy of CRT (10 nM) solution as a function of J6f5 RNA concentration.

to understanding the underlying recognition rules for RNA−aminoglycoside binding. As stated above, micromolar binding affinities are routine for aminoglycoside−RNA binding, and may not involve any highly specific interactions. For example, we have found that various commercially available tRNA molecules all bind aminoglycosides with micromolar affinities (Wang and Rando, unpublished experiments).

The J6 tobramycin binding aptamer has been studied with respect to the minimal structural unit capable of high-affinity and specific aminoglycoside binding. Previously performed affinity cleavage studies, using tobramycin−iron/EDTA analogs, showed that J6 and other tight binding aptamers were all cleaved at their consensus sequence regions (Wang et al., 1996). Secondary structure predictions suggested that the consensus regions are located in stem−loops (Wang & Rando, 1995; Wang et al., 1996). Experiments reported here using RNases T1 and U2 are quite consistent with the secondary structure of J6 as predicted by Mfold (Jaeger et al., 1991).

The experiments discussed above show that the putative stem−loop regions are important components of the aminoglycoside binding site, but they do not demonstrate that aminoglycoside binding is confined to the stem−loops. This issue can be addressed quantitatively, because J6 binds tobramycin with a $K_D = 0.77 \pm 0.03$ nM, and differentiates between structurally similar aminoglycosides by factors of 10^3−10^4. Note the substantial differences in the binding of the very similar kanamycin B to that of tobramycin (Table 2).

Initial experiments designed to simplify J6 centered on using restriction enzymes to cleave the J6 DNA from the 3′ end. Runoff transcripts generated J6a (87-mer), J6b (71-mer), and J6c (57-mer). These truncated versions of J6 showed lower affinities for tobramycin by factors of 20−30 when compared to J6 itself. While the truncated J6s could still differentiate between the various aminoglycosides, their specificities were less impressive than that found with J6. J6c was further simplified by deleting 11 and 19 nts from the 5′ end to generate J6d and J6e, respectively. J6d, the 47-mer, was unable to bind aminoglycosides. However, a secondary structure prediction using Mfold (Jaeger et al., 1991) suggested that the structure of this construct was radically different from the usual J6 stem−loop structures. Interestingly, J6e (39-mer) was again able to specifically bind aminoglycosides, but with a diminished $K_D = 58.2 \pm 13.1$ nM for tobramycin, by comparison with the other stem–loop aminoglycoside binding constructs. Because of the floppy ends of J6e, an additional terminal GC base pair was added to produce J6e1, which bound tobramycin with a $K_D = 15.6 \pm 1.5$ nM. Finally, substitution of a U for a G near the 5′ end generated another GC base pair in J6f1, which now bound tobramycin with a $K_D = 5.15 \pm 1.52$ nM. Whether the crude notion of tightening up the structure by the addition of GC base pairs has any meaning at all remains to be seen; nevertheless, the aminoglycoside binding specificity and affinity of J6f1 are impressive given its size compared to J6. J6f1 is, of course, an ideal candidate for structural studies because it shows high affinity and stoichiometry of aminoglycoside binding.

Another interesting aspect of the work on the truncated structures relates to the studies on J6e2, J6f2, and J6f3 in which the putative bulges of J6e1 or J6f1 were deleted. Quantitative binding studies on J6e2, J6f2, and J6f3 showed that they only weakly and nonspecifically bound aminoglycosides. Therefore, these two bulges are essential for specific aminoglycoside binding. Elimination of the trinucleotide bulge and the single A bulge decreases binding affinities markedly, and the 1:1 stoichiometry of binding is lost. The trinucleotide bulge and the single A bulge could be important with respect to governing the overall structure of the construct and/or they could be part of the tobramycin binding site. Moreover, the studies on J6f4 and J6f5, which have four-base loops instead of the original six-base loop, show that the consensus stem–loop is essential for tight and stoichiometric aminoglycoside binding. Structural studies on J6f1 and similar constructs should reveal in what ways the trinucleotide bulge, the single A bulge, and six-base loop are important for high-affinity tobramycin binding. Further probing of the small high affinity constructs will reveal the essential structural elements required for specific and high-affinity tobramycin binding.

REFERENCES

Aziz, R. B., & Soreq, H. (1990) *Nucleic Acids Res. 18*, 3418.
Chambers, H. F., & Sande, M. A. (1996) *Goodman & Gilman's The Pharmacological Basis of Therapeutics*, p 1103, McGraw Hill Companies, New York.
Chernoff, Y. O., Vincent, A., & Liebman, S. W. (1994) *EMBO J. 13*, 906–913.
De Stasio, E. A., & Dahlberg, A. E. (1990) *J. Mol. Biol. 212*, 127–133.
Fourmy, D., Recht, M. I., Blanchard, S. C., & Puglisi, J. D. (1996) *Science 274*, 1367–1371.
Jaeger, J. A., Turner, D. H., & Zuker, M. (1989) *Methods Enzymol. 183*, 281–306.
Lato, S. M., Boles, A. R., & Ellington, A. D. (1995) *Chem. Biol. 2*, 219–303.
Noller, H. F. (1991) *Annu. Rev. Biochem. 60*, 191–227.
Purohit, P., & Stern, S. (1994) *Nature 370*, 659–662.
von Ahsen, U., & Noller, H. F. (1993) *Science 260*, 1500–1503.
von Ahsen, U., Davis, J., & Schroeder, R., (1991) *Nature 353*, 368–370.
Wallis, M. G., von Asen, U., Schroeder, R., & Famulok, M. (1995) *Chem. Biol. 2*, 543–552.
Wang, Y., & Rando, R. R. (1995) *Chem. Biol. 2*, 281–290.
Wang, Y., Killian, J., Hamasaki, K., & Rando, R. R. (1996) *Biochemistry 35*, 12338–12346.
Wang, Y., Hamasaki, K., & Rando, R. R. (1997) *Biochemistry 36*, 768–779.

BI971095T